adap-org/9505004

Hydrodynamic effects in density waves of granular flows

Kengo Ichiki *
Department of Physics, Tohoku University, Sendai 980-77, Japan
(ay 29, 1995)

Abstract

Granular flows in a narrow pipe are studied numerically by the model taking account of hydrodynamic effects of fluid surrounding particles. In the simulations density waves are observed over the wide range of the Stokes number, which represents the inertial effect of particles. The mechanisms of formation of the density waves are considered and two types of density waves, which are observed in the systems with zero and finite Stokes numbers, are presented. Power spectra of density waves obtained from the simulations with non-zero Stokes number show $1/f^{\alpha}$ power law which is similar to that in experiments.

46.10.+z,47.55.Kf,05.40.+j

Typeset using REVTEX

*Electronic address: ichiki@cmpt01.phys.tohoku.ac.jp

Granular materials are not only important in technology and industry, but also are very familiar to us. We can see them in daily life, for example, sugar and salt in kitchen, sandy beach and soil on which we live. Although these granular materials consist of simple components which are granular particles and surrounding fluid, they show a large variety of phenomena and attract a lot of interests of scientists [1–6]. During the last decade, many people have studied a lot of subjects on granular flows such as vibrating beds [7–9], fluidized beds [10–12], hopper flows [13,14], pipe flows [15–19], and so on.

Pipe flow, which we discuss in this paper, seems to be the simplest system of them, in which granular particles is falling in a narrow pipe. Even in such a simple system, it is observed in experiments that the uniform flow of particles is unstable and density waves appear [15,16,19]. In addition the fluctuation of density show $1/f^{\alpha}$ spectra [15,19]. By numerical simulations assuming mechanical dissipations such as roughness of walls and inelasticity of collisions, the creation of density waves [16–18] and the appearance of $1/f^{\alpha}$ spectra [18] were reported. Studies of the clustering behavior of inelastic particles [20,21] are in the same context.

However one can expect naturally that the hydrodynamic effects of fluid surrounding particles must play an important role in the phenomena. It is sufficient to remember a simple example that one particle is falling down by the gravity. Situation is more difficult in the pipe flows because the hydrodynamic effects depend on the density of particle significantly [22]. Recently the present author and Hayakawa have constructed a model of granular particles that takes account of the hydrodynamic effects by applying the method of the Stokesian dynamics [23], and have succeeded to create realistic bubbling and slugging flows in fluidized beds [12].

The aim of this paper is to apply this model to the problems of pipe flows and to demonstrate the importance of the hydrodynamic effects.

Since the simulation method used in this paper is described in detail in Ref. [12], we briefly summarize the method. Particles are driven by the gravity, hydrodynamic force from surrounding fluid and hard-core interaction in direct collisions between particles. The equation of motion of particle α is given as

$$St\frac{d}{dt}\mathbf{v}^{(\alpha)} = \mathbf{F}_f^{(\alpha)} - \mathbf{e}_z, \tag{1}$$

where $\mathbf{v}^{(\alpha)}$ is the velocity of particle α, $\mathbf{F}_f^{(\alpha)}$ is the hydrodynamic force, $-\mathbf{e}_z$ is the unit vector directed to the gravity and $St = mU_0/6\pi\mu a^2$ is the Stokes number. In this paper we assume that all particles have same radius a and the mass m. In Eq. (1), quantities are nondimensionalized by the length a and one-particle sedimentation velocity $U_0 = m\tilde{g}/6\pi\mu a$, where $\tilde{g}$ is effective gravitational acceleration corrected by buoyancy and μ is the viscosity of the fluid. Direct collisions between particles are considered to be elastic. Particles interact with others through the hydrodynamic force which includes the many body effects of particle configuration. In low Reynolds number limit, where the viscosity is dominant, $\mathbf{F}_f^{(\alpha)}$ can be written in the matrix form as

$$\mathbf{F}_f^{(\alpha)} = -\sum_{\beta} \mathsf{R}^{(\alpha\beta)} \cdot \mathbf{v}^{(\beta)}, \tag{2}$$

where R is so called resistance matrix scaled by $6\pi\mu a$. As described in Ref. [12], the resistance matrix is constructed by the procedure of Stokesian dynamics [23] with periodic boundary

TABLE I. The parameters of simulations. St' is the effective Stokes number in Eq. (3), N is the number of particles in the unit cell, L_x,L_y and L_z are the lengths of the unit cell.

	St'	N	L_x	L_y	L_z
(a)	0.0	30	6	2	80
(b)	10.0	30	6	2	80
(c)	100.0	30	6	2	80
(d)	10.0	15	6	2	80
(e)	∞	30	6	2	80

condition [24]. Here we neglect the rotation of particles for simplicity. In addition, we approximate (1) and (2) as follows,

$$St' \frac{d}{dt} \mathbf{v}^{(\alpha)} = \mathbf{v}_t^{(\alpha)} - \mathbf{v}^{(\alpha)}, \tag{3}$$

$$-\mathbf{e}_z = \sum_\beta \mathsf{R}^{(\alpha\beta)} \cdot \mathbf{v}_t^{(\beta)}, \tag{4}$$

where $\mathbf{v}_t$ denotes the terminal velocity. This approximation means that we neglect many body effects only in the relaxation process of particle velocity to the terminal velocity. In this sense, St' should be treated as the effective Stokes number.

In the simulation, we use narrow cells with periodic boundary condition. For computational efficiency we only discuss the results on monolayer simulations where particles in each unit cell can move only on the plane parallel to the direction of gravity and the width of the cell is equal to the diameter of particles. In fact there is no qualitative difference between the monolayer and full three-dimensional simulations. All simulations presented in this paper are calculated as follows. Particles are settled randomly with no initial velocities and the evolution obeys the equation of motion and the collision law. In Table I the parameters used in the simulations are summarized.

At first we investigate the effect of St' which is the inertial effect of particles and the only parameter in our model. Spatiotemporal patterns of density are shown in Fig. 1 (a),(b) and (c), where St' is equal to 0, 10 and 100 respectively. We choose the other parameters as the number of particles in the unit cell $N = 30$ and the cell lengths $(L_x, L_y, L_z) = (6a, 2a, 80a)$. The figure shows that uniform state is unstable in all case. We can also observed that one sharp cluster are formed and the internal motions of particles in the cluster almost freeze in $St' = 0$ and otherwise broader cluster appears. We note that small (large) St' corresponds to the fluid with high (low) viscosity like water (air). This means that in not only air but also water density waves can be observed.

Let us consider the mechanisms of dynamics of this behavior. Our model consists of three types of mechanisms: inertial effects of particles, hydrodynamics interactions and hard-core collisions. From the macroscopic point of view, the inertial effect and the collisions cause the advection and the diffusion of particles. Hydrodynamic effect is realized as the mean velocity of particles depending on the local density, which is in general decreasing function of the density. Therefore only the collisions can have the stabilizing effect on the disturbance of density. We define the kinematic regime and the dynamic regime which are correspond to the cases where St' is zero and finite respectively. In the kinematic regime (Fig. 1

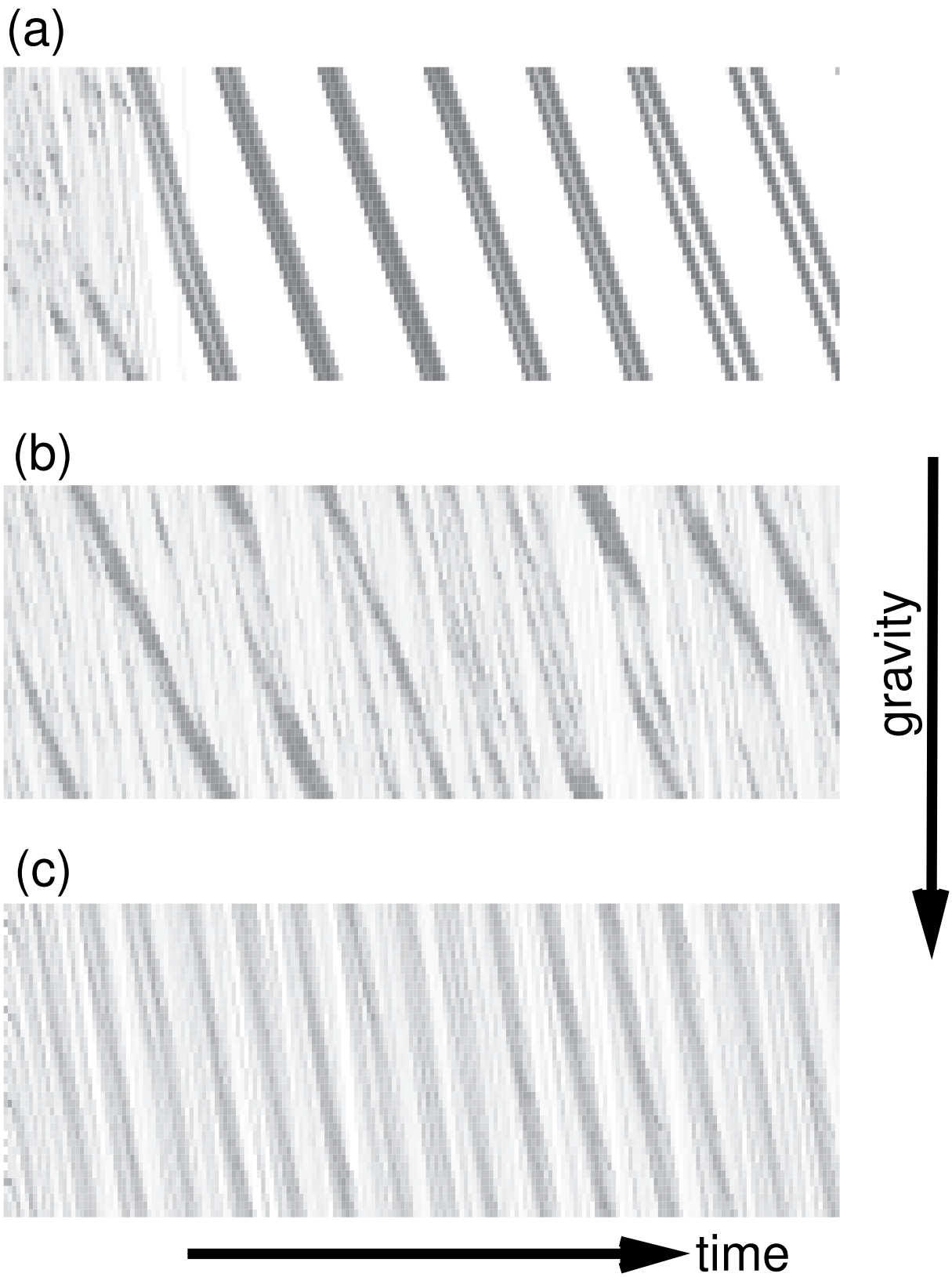

FIG. 1. Spatiotemporal patterns of density for the first 6000 scaled time with (a) $St' = 0$,(b) $St' = 10$ and (c) $St' = 100$. Other parameters are listed in Table I. Dark regions correspond to high densities.

TABLE II. The characteristic velocities and frequencies and the exponents of power laws. V_c and $\bar{V}$ is scaled by one-particle sedimentation velocity U_0, and f_c and f_s is scaled by the lowest frequency f_0.

	V_c	$\bar{V}$	f_c	f_s	α
(b)	0.12	0.28	8	350	$-1.47 \pm 3 \times 10^{-2}$
(c)	0.21	0.31	13	380	$-1.40 \pm 3 \times 10^{-2}$
(d)	0.18	0.43	11	510	$-1.32 \pm 3 \times 10^{-2}$

(a)), dynamical effects such as the advection and the collisions vanish and then systems are completely governed by (4). On the other hand in the dynamic regime (Fig. 1 (c)), the dynamical effects dominate. The regime in Fig. 1 (b) may be the intermediate regime where both effects are important.

We vary parameter N fixing $St' = 10$ in order to examine the dependence of density wave on the particle density. If the number of particles become large ($N = 60$), internal motions of particles is weakened. Thus dynamical effects are suppressed and particles are almost frozen in cluster like in the case of $St' = 0$. If the number of particles becomes small ($N = 15$), which is (d) in Table I, density waves seem to be unstable though they are observed.

Let us examine the effect of wall confining fluid and particles. For this purpose, we introduce the fixed particles which form vertical wall. It is found from the simulation that the wall enhances the horizontal motions and the collisional effects when St' is finite. The system with wall behaves like that without wall but with larger St'.

Next we investigate the power spectra obtained from the simulations in Table I (Fig. 2). These spectra are calculated as follows. At first we divide horizontally the unit cell into 20 sub cells and calculate the time series of density in each sub cell. Then we calculate the power spectra of each sub cell by a fast Fourier transform with the Parzen window for the last 16384 time series of the simulation and average them over 20 sub cells. Frequencies are scaled by f_0 which is the lowest frequency. The simulation (e) is presented as the example with no density waves for comparison, which correspond to the case of $St' = \infty$ and is performed without the hydrodynamic effects and the gravity but with the initial velocity as their terminal velocities in the case of $St' = 10$. We can see that power laws are observed for the simulations with finite St' in the range between $f_c = V_c/L_z$ and $f_s = \bar{V}/4a$, where V_c and $\bar{V}$ are the mean velocity of the cluster and the particles respectively, L_z is system size in direction of the gravity and $4a$ is the length of the sub cells used in the calculation of spectra. Therefore f_c and f_s correspond to the return time of cluster and the characteristic time in small scale motion respectively. The exponents in the range are shown in Table II.

This kind of spectra of density fluctuation have been observed in hourglass twenty years ago [15]. In a recent experiment of pipe flow [19], similar power spectra have been obtained and the high-frequency limit in them may corresponds to f_s in this simulation. From the meaning of f_c and f_s, it is suggested that the power law reflects the behavior in relatively small scale rather than the cluster itself. The existence of low-frequency limit in Fig. 2 may be due to the limit of system size or the periodicity in the simulations. Therefore we need to construct the model without periodic boundary condition in order to investigate the behavior of larger scale like clusters and the relation to the real systems.

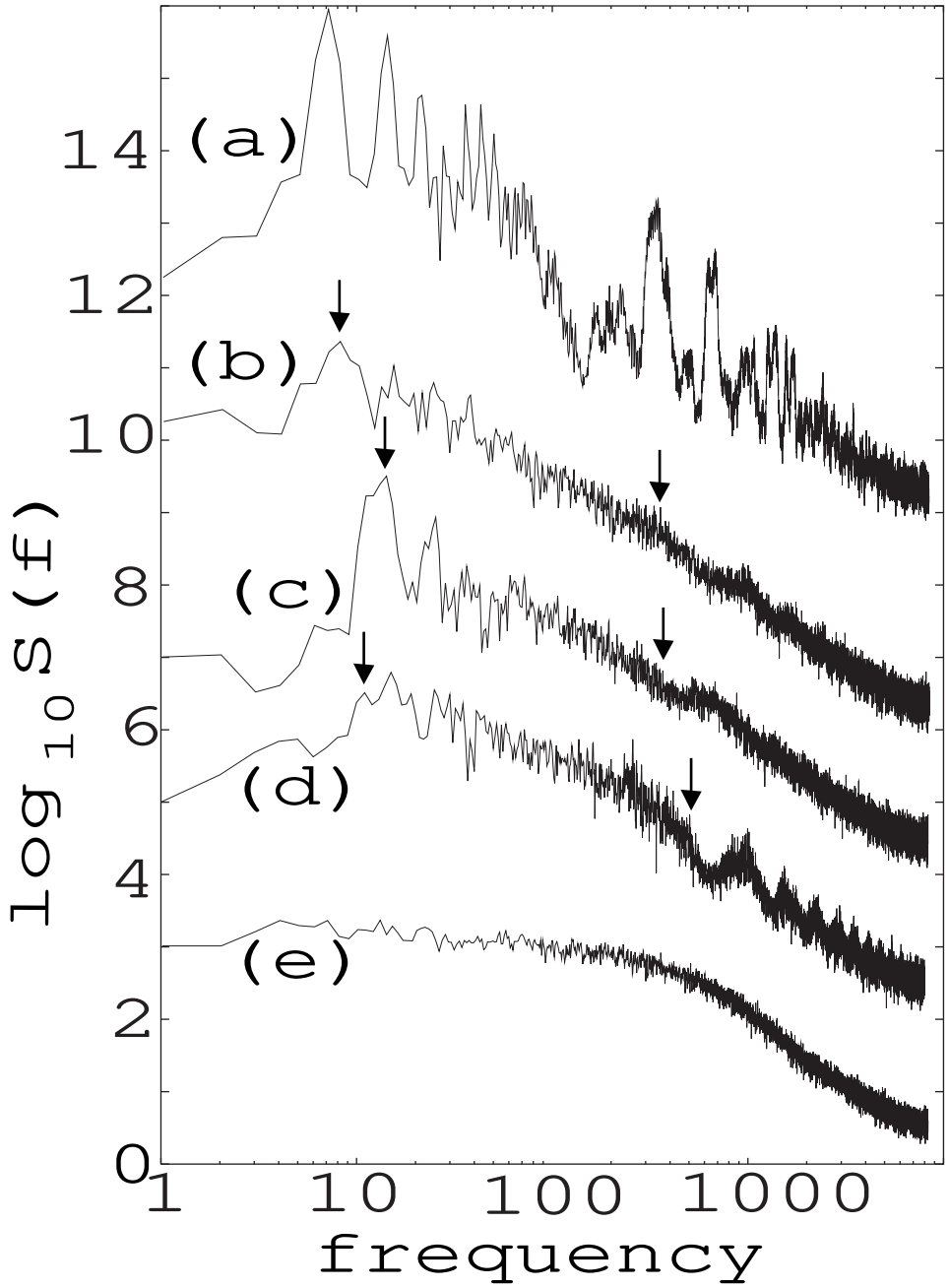

FIG. 2. Power spectra $S(f)$ of density fluctuation of the simulations in Table I. These spectra are calculated by a fast Fourier transform with the Parzen window. Frequency is scaled by the lowest one. Arrows correspond to f_c and f_s in Table II.

In conclusion, by means of the numerical simulations [12], it is found that in pipe flows the hydrodynamic effects of the fluid surrounding particles play an important role and density waves appear in the wide range of St. This means that in the water as well as in the air density waves can be observed. Two mechanisms to form density waves, which are inertial effects of particles and the hydrodynamic interactions, are suggested. In the case of finite St', $1/f^{\alpha}$ power laws, which may represent the behavior of particles falling from the cluster, are observed.

Finally we note that there are a lot of resemblances between the pipe flows and the traffic flows in an expressway. The kinematic waves have been studied as the model of traffic flows [25]. In addition our model is formally similar to the model of traffic flows presented in Ref. [26] and $1/f$ power spectra are also observed in the real traffic [27] and in the numerical model [28].

The author thanks Hisao Hayakawa and Toshio Tsuzuki for stimulating discussions, Yoshi-hiro Taguchi, Akio Nakahara and Mitsugu Matsushita for helpful comments and encouragements and Teruhisa S. Komatsu for useful suggestion on the resemblance to traffic flow. Most of simulations in this paper have been done using the facilities of the Supercomputer Center, Institute of Solid State of Physics, University of Tokyo.

REFERENCES

[1] H. M. Jaeger and S. R. Nagel, Science **255**, 1523 (1992).

[2] Y-h. Taguchi, H. Hayakawa, S. Sasa, and H. Nishimori eds., Int. J. Mod. Phys. B **7**, 1757 (1993).

[3] *Disorder and Granular Media*, edited by D. Bideau and A. Hansen (North-Holand, Amsterdam, 1993).

[4] *Powders and Grains 93*, edited by C. Thornton (Balkema, Rotterdam, 1993).

[5] *Granular Matter – An Interdisciplinary Approach*, edited by A. Metha (Springer-Verlag, New York, 1993).

[6] H. Hayakawa, H. Nishimori, S. Sasa, and Y-h. Taguchi, Jpn. J. Appl. Phys. **34**, 397 (1995).

[7] P. Evesque and J. Rajchenbach, Phys. Rev. Lett. **61**, 44 (1989).

[8] Y-h. Taguchi, Phys. Rev. Lett. **69**, 1367 (1992).

[9] J. A. C. Gallas, H. J.Herrmann, and S. Sokołowski, Phys. Rev. Lett. **69**, 1371 (1992).

[10] *Fluidization*, 2nd ed., edited by J. F. Davidson, R. Clift, and D. Harrison (Academic Press, London, 1985).

[11] D. Gidaspow, *Multiphase Flow and Fluidization* (Academic Press, London, 1994).

[12] K. Ichiki and H. Hayakawa, Phys. Rev. E (1995), to be published. (chao-dyn/9502021).

[13] G. W. Baxter, R. P. Behringer, T. Fagert, and G. A. Johnson, Phys. Rev. Lett. **62**, 2825 (1989).

[14] G. H. Ristow and H. J. Herrmann, Phys. Rev. E **50**, R5 (1994).

[15] K. L. Schick and A. A. Verveen, Nature **251**, 599 (1974).

[16] T. Pöschel, J. Phys. I France **4**, 499 (1994).

[17] J. Lee, Phys. Rev. E **49**, 281 (1994); J. Lee and M. Leibig, J. Phys. I France **4**, 507 (1994).

[18] G. Peng and H. J. Herrmann, Phys. Rev. E **49**, R1796 (1994); **51**, 1745 (1995).

[19] S. Horikawa, A. Nakahara, T. Nakayama, and M. Matsushita, (1995), submitted to J. Phys. Soc. Jpn.

[20] I. Goldhirsch and G. Zanetti, Phys. Rev. Lett. **70**, 1619 (1993).

[21] S. McNamara and W. R. Young, Phys. Rev. E **50**, R28 (1994).

[22] H. Hayakawa and K. Ichiki, Phys. Rev. E **51**, R3815 (1995).

[23] J. F. Brady and G. Bossis, Annu. Rev. Fluid Mech. **20**, 111 (1988).

[24] C. W. J. Beenakker, J. Chem. Phys. **85**, 1581 (1986).

[25] M. J. Lighthill and G. B. Whitham, Proc. R. Soc. Lond. A **229**, 317 (1955); G. B. Whitham, *Linear and Nonlinear Waves* (John Wiley & Sons, New York, 1974).

[26] M. Bando *et al.*, Jpn. J. Ind. Appl. Math. **11**, 203 (1994); Phys. Rev. E **51**, 1035 (1995).

[27] T. Musha and H. Higuchi, Jpn. J. Appl. Phys. **15**, 1271 (1976); **17**, 811 (1978).

[28] K. Nagel and M. Paczuski, Phys. Rev. E **51**, 2909 (1995).